

Supporting information for

Induced Charge Electro-osmotic Particle Separation

Xiaoming Chen¹, Yukun Ren^{*1,2,3}, Likai Hou¹, Xiangsong Feng¹, Tianyi Jiang¹, and Hongyuan Jiang^{*1,2}

1. School of Mechatronics Engineering, Harbin Institute of Technology, Harbin 150001, PR China

2. State Key Laboratory of Robotics and System, Harbin Institute of Technology, Harbin 150001, PR China

3. State Key Laboratory of Nonlinear Mechanics, Chinese Academy of Sciences, Beijing 100190, PR China

Section 1. Boundary conditions of induced charge electro-osmotic particle separation

Section 2. Definitions of the focusing width and focusing distance

Section 3. The focusing characterizations of PMMA micro-beads

Section 4. The focusing characterizations of PS2 micro-beads

Section 5. The focusing characterizations of yeast cells

Section 1. Boundary conditions of induced charge electro-osmotic particle separation.

The ICEO slip velocity on the floating electrode is calculated using^{1, 2}

$$\langle \mathbf{u}_s \rangle = \frac{\varepsilon}{2(1+\delta)\eta} \operatorname{Re} \left(\left(\frac{\phi_0 A_1}{2} \right) (\mathbf{E}_0 \mathbf{E}_0 \mathbf{n} \cdot \mathbf{n})^* \right) \quad (1)$$

The slip velocities applied on the left and right driving electrodes are given by

$$\langle \mathbf{u}_s \rangle = \frac{\varepsilon}{2(1+\delta)\eta} \operatorname{Re} \left(\left(\frac{\phi_0 A_1}{2} \right) (\mathbf{E}_0 \mathbf{E}_0 \mathbf{n} \cdot \mathbf{n})^* \right) \quad (2)$$

$$\langle \mathbf{u}_s \rangle = \frac{\varepsilon}{2(1+\delta)\eta} \operatorname{Re} \left(\left(\frac{\phi_0 A_1}{2} \right) (\mathbf{E}_0 \mathbf{E}_0 \mathbf{n} \cdot \mathbf{n})^* \right) \quad (3)$$

where $\phi_0 = A e^{j\vartheta}$ is a complex phasor amplitude of the electrostatic potential $\phi(t) = A \cos(\omega t + \vartheta)$ ($j = \sqrt{-1}$ and $\omega = 2\pi f$ is the angular frequency); η the dynamic viscosity of electrolyte; $\mathbf{E}_0 = -\nabla \phi_0$ the electric field phasor; ε electrolyte permittivity; δ the ratio C_d / C_s (C_d the capacitance of diffuse layer, C_s the capacitance of the stern layer); $\langle \mathbf{u}_s \rangle$ the time-averaged ICEO slip velocity; $\operatorname{Re}(\dots)$ the real part of (\dots) ; and \mathbf{n} the unit normal vector pointing into the electrolyte. An asterisk denotes complex conjugation.

The other boundaries in the numerical model are set as a no-slip wall. By substituting the foregoing boundary conditions into the governing equation, i.e., the Navier–Stokes equation, the fluid flow distribution in the model can be obtained. From the equation of motion for the particles,³

$$m_p \frac{du_i}{dt} = 6\pi a \mu (v_i - u_i) + (m_p - m_f) g_i + F_i^{DEP} \quad (4)$$

we obtain the trajectory of each particle numerically. Each particle type has its unique trajectory under the ICEO effect.

Section 2. Definitions of the focusing width and focusing distance

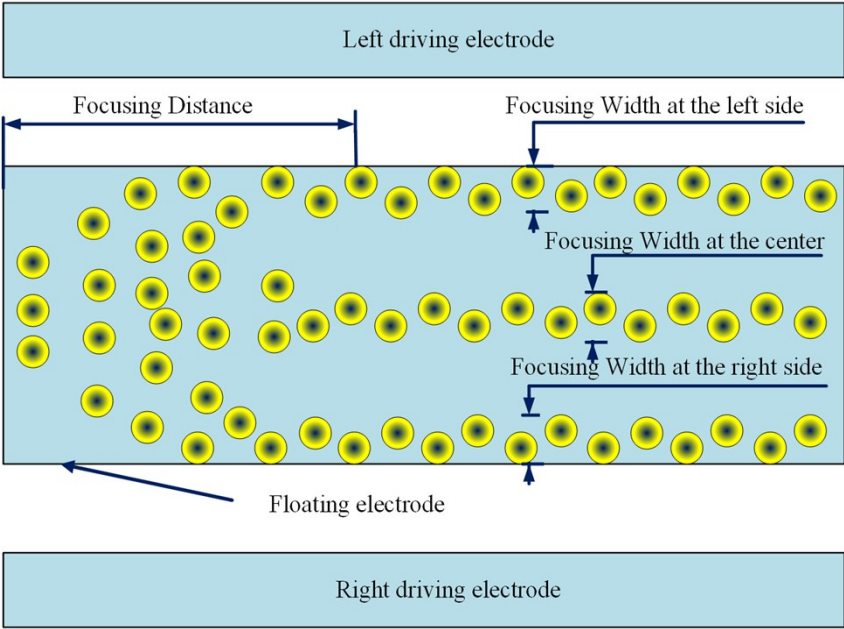


Fig. S1 Schematic diagram defining the focusing width and focusing distance of the manipulated particles on the floating electrode.

Section 3. The focusing characterizations of PMMA micro-beads

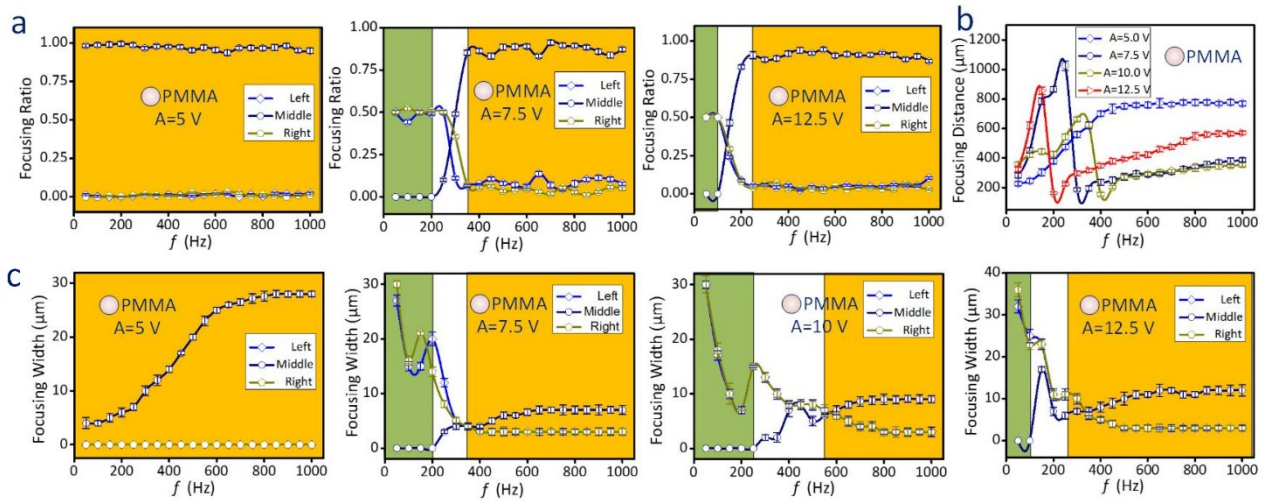


Fig. S2 The focusing characterizations of PMMA micro-beads. (a) The plots of the focusing ratio against frequency at $A=5\text{ V}$, 7.5 V , 12.5 V . (b) The curves illustrating the relationship between the focusing distance and frequency under different voltage intensity. (c) Plots demonstrating the dependence of the focusing width on frequency (The green/orange backgrounds indicate the frequency ranges that almost all the PMMA micro-beads are focused at the both sides/center of floating electrode).

Section 4. The focusing characterizations of PS2 micro-beads

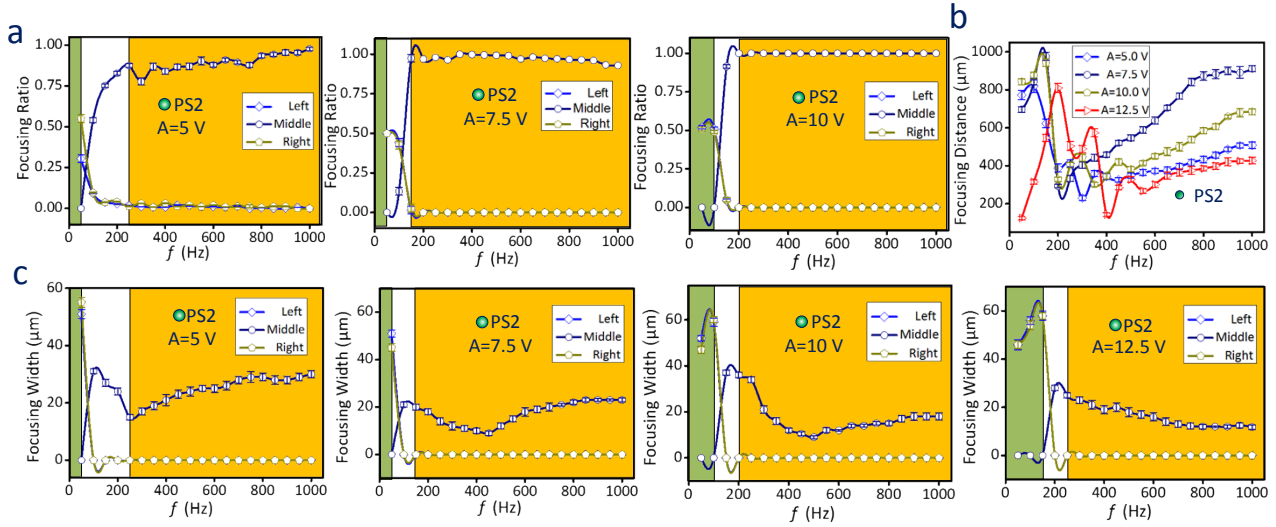


Fig. S3 The focusing characterizations of PS2 micro-beads. (a) The plots of the focusing ratio against frequency at $A=5$ V, 7.5 V, 10 V. (b) The curves illustrating the relationship between the focusing distance and frequency under different voltage intensity. (c) Plots demonstrating the dependence of the focusing width on frequency (The green/orange backgrounds indicate the frequency ranges that almost all the PS2 micro-beads are focused at the both sides/center of floating electrode).

Section 5. The focusing characterizations of yeast cells

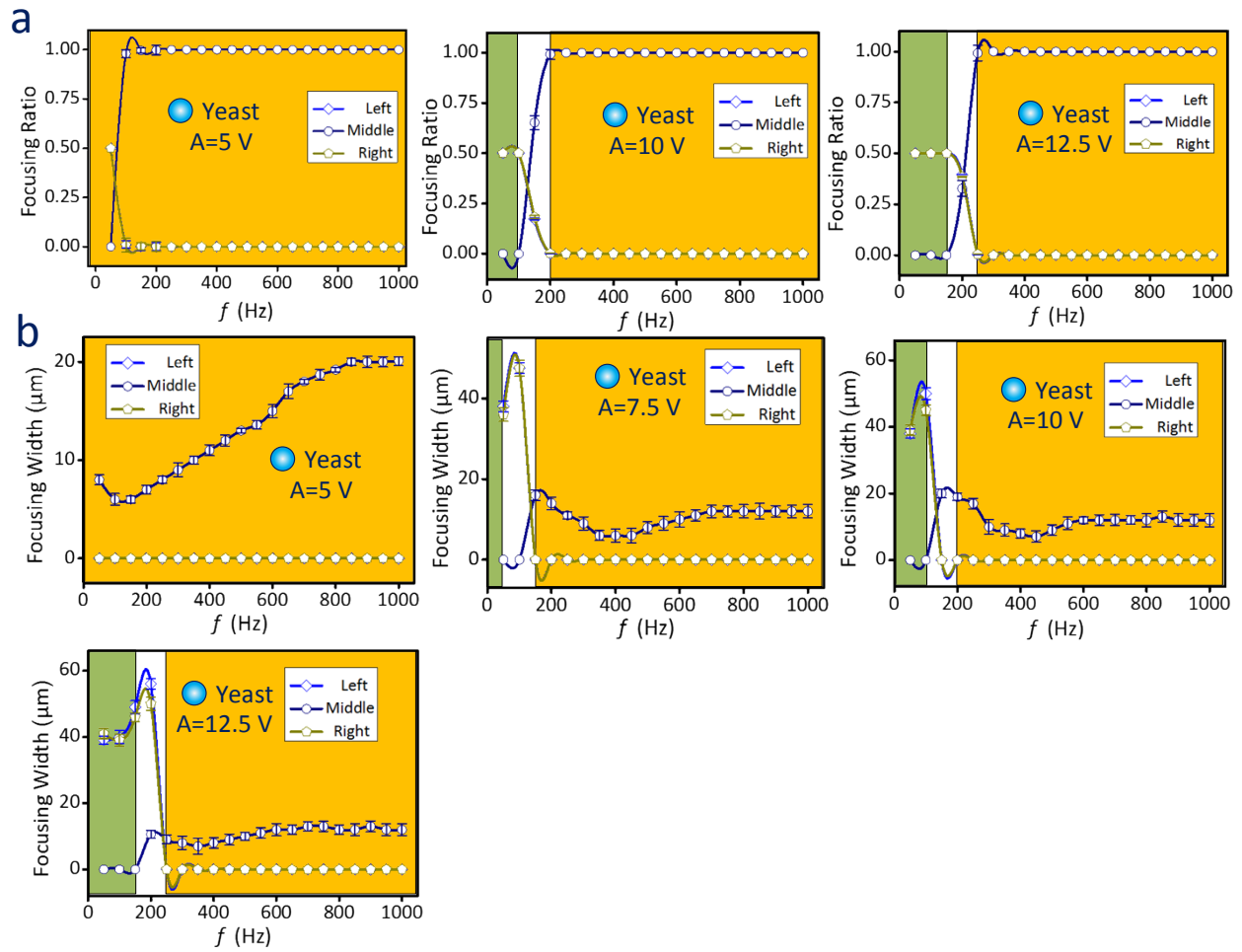


Fig. S4 The focusing characterizations of yeast cells. (a) The plots of the focusing ratio against frequency at $A=5\text{ V}$, 10 V , 12.5 V . (b) Plots demonstrating the dependence of the focusing width on frequency (The green/orange backgrounds indicate the frequency ranges that almost all the yeast cells are focused at the both sides/center of floating electrode).

Reference

1. Y. Ren, W. Liu, Y. Jia, Y. Tao, J. Shao, Y. Ding and H. Jiang, *Lab on a chip*, 2015, **15**, 2181-2191.
2. T. M. Squires and M. Z. Bazant, *Journal of Fluid Mechanics*, 2004, **509**, 217-252.
3. Y. Ren, X. Liu, W. Liu, Y. Tao, Y. Jia, L. Hou, W. Li and H. Jiang, *Electrophoresis*, 2018, **39**, 597-607.